

## **General Disclaimer**

### **One or more of the Following Statements may affect this Document**

- This document has been reproduced from the best copy furnished by the organizational source. It is being released in the interest of making available as much information as possible.
- This document may contain data, which exceeds the sheet parameters. It was furnished in this condition by the organizational source and is the best copy available.
- This document may contain tone-on-tone or color graphs, charts and/or pictures, which have been reproduced in black and white.
- This document is paginated as submitted by the original source.
- Portions of this document are not fully legible due to the historical nature of some of the material. However, it is the best reproduction available from the original submission.

(NASA-CR-150383) M551 METALS MELTING  
EXPERIMENT Final Report (Grumman Aerospace  
Corp.) 29 p HC A03/MF A01 CSCL 22A

N77-31214

Unclas  
G3/12 47392

RE-536

M551 METALS MELTING EXPERIMENT

January 1977

RESEARCH DEPARTMENT



GRUMMAN AEROSPACE CORPORATION  
BETHPAGE NEW YORK

2/16/77

Grumman Research Department Report RE-536

M551 METALS MELTING EXPERIMENT

Prepared by

G. Busch

Research Department  
Grumman Aerospace Corporation  
Bethpage, New York 11714

for

George C. Marshall Space Flight Center  
National Aeronautics and Space Administration  
Marshall Space Flight Center, Alabama 35812

Final Report on Contract NAS 8-28728 Mod. 6

January 1977

Approved by:

*Charles E. Mack, Jr.*

Charles E. Mack, Jr.  
Director of Research

## ABSTRACT

In the Skylab M551 metals melting experiment, electron beam welding studies were conducted on three different materials; namely, 2219-T87 aluminum alloy, 304L stainless steel, and commercially pure tantalum (0.5 wt % columbium). Welds were made in both one gravity and zero gravity (Skylab) environments. Segments from each of the welds were investigated by microhardness, optical microscopy, scanning microscopy, and electron probe techniques. The macrostructural and microstructural features observed in the welds served as a basis for conducting the scanning microscope and microprobe studies. For example, in all the 2219-T87 aluminum alloy samples, macroscopic banding and the presence of a eutectic phase in the grain boundaries of the heat affected zone were observed. Subsequent microprobe studies showed that inverse segregation in the fusion zone and the segregation of copper was greater in the Skylab sample than in the comparable ground base sample. All the stainless steel samples exhibited a sharp weld interface and macroscopic bands. As a result, the variations in microchemistry in these areas were explored. The primary microstructural features found in the tantalum samples is the presence of either columnar grains (ground base) or equiaxed grains (Skylab). Microchemical studies of these samples showed that ground base samples exhibited normal macrosegregation in the weld, i.e., increasing solute concentration at the center of the fusion zone. The Skylab samples, on the other hand, were uniform in concentration and did not exhibit any macrosegregation. The factors contributing to these effects are discussed and the role of reduced gravity in welding is considered.

## TABLE OF CONTENTS

<u>Item</u>	<u>Page</u>
INTRODUCTION . . . . .	1
EXPERIMENTAL PROCEDURES . . . . .	1
ANALYTICAL RESULTS AND DISCUSSIONS . . . . .	2
Macrostructure . . . . .	2
2219-T87 Aluminum Alloy . . . . .	3
Tantalum - 0.5 wt % Columbium . . . . .	12
304L Stainless Steel . . . . .	15
CONCLUSIONS . . . . .	23
FUTURE WORK . . . . .	24
ACKNOWLEDGEMENTS . . . . .	24
REFERENCES . . . . .	24

## LIST OF ILLUSTRATIONS

<u>Figure</u>		<u>Page</u>
1	Variations in Microhardness of a Weld Segment From the 2219 Aluminum Alloy Disc Processed Aboard Skylab	4
2	A comparison of Growth Patterns in the Crown Sections of the Aluminum Alloy (2219) Weld	5
3	Cross Sections of the Aluminum Alloy Welds Illustrating Variation in Thickness of the Fine Grain Chill Zone	6
4	A Comparison of Dendrite Shape and Size in the Aluminum Alloy Welds	8
5	Variation in the Average Copper Concentration Along the Center Line of the Ground Base Weld	10
6	Variation in the Average Copper Concentration Along the Center Line of the Skylab Weld	11
7	A Comparison of Solidification Patterns in the Crown Sections of Thin Cross Section Tantalum Welds	13
8	A Comparison of Solidification Patterns in the Crown Sections of Large Cross Section Tantalum Welds	14
9	Variation in Microchemistry Across the Heat Affected Zone and Weld Metal in Ground Base Sample No. 11	16
10	Variation in Microchemistry Across the Heat Affected Zone and Weld Metal of Skylab Sample No. 11	17
11	Schematic of the Variations in Microchemistry of Individual Grains in the Tantalum Alloy Weld	18
12	Solidification Modes Found in Stainless Steel Alloy Welds a) Plane Front and Cellular b) Cellular Dendrites	20
13	Schematic of the Variations in Microchemistry at the Weld Interface in the Stainless Steel Welds	21
14	Schematic of the Microchemistry Changes Across a Band in the Stainless Steel Welds	22

## INTRODUCTION

The M551 (Metals Melting) Skylab experiment consisted of sequentially melting three rotating discs with an electron beam. The discs were made of a 2219-T87 aluminum alloy, 304L stainless steel, and commercial grade tantalum (0.5 wt % columbium). In order to determine if any differences occurred as a result of welding in space, three similar discs were melted in a similar electron beam facility on earth. This investigation is a continuation of the characterization of the specimens begun by McKannan and others (Refs. 1-3).

The electron beam unit used for the melting experiment was operated at 20 kV and 50 to 80  $\mu$ A. In these studies the beam was positioned 6 cm from the plane of the disc and normal to it. The discs were rotated, so that the tangential velocity at the point of impingement of the beam was 1.61 cm/sec. At the conclusion of the flight the three discs were returned to the Marshall Space Flight Center for evaluation.

## EXPERIMENTAL PROCEDURES

Representative samples of each weld material generated in the experiment were received from NASA Marshall Space Flight Center in standard metallurgical mounts. The 2219-T87 aluminum alloy and the 304L stainless steel were repolished with alumina. The hardness surveys were conducted with a Reichert microhardness tester, which was calibrated in the following manner. First, the length constant for the optical system was calculated. After zeroing the weight scale, the deflection scale was calibrated using a standard series of weights from 5 to 100 grams. A plot of the scale deflection vs applied weight agreed very well with the factory calibration curve. Hardness traverses on the samples were then made using either 50 or 100 gram loads applied for 30 seconds. Two traverses were usually made on both the cross and crown sections. Hardness measurements were made 0.24 mm apart, except at the weld interfaces where they were made 0.1 mm apart.

The diagonals of the diamond indentation were measured in both directions, averaged, and converted to micrometers. From these values, the microhardness ( $H_m$ ) was determined according to the following formula

$$H_m = 1834.4 \frac{P}{d^2} \text{ Kg/mm}^2$$

where P is the load in grams and d is the diagonal length in mm.

At the conclusion of the hardness surveys the samples were etched for further microstructural studies. The following etchants were used:

<u>Alloy</u>	<u>Etchant</u>	<u>Features Revealed</u>
2219-T87 A1	10ml $H_3PO_4$ , 90ml $H_2O$ (50°C)	Eutectic and rosette structure
	Kellers etch	General grain size and shape
304L SS	40ml $HNO_3$ , 10ml $HCl$ , 40ml Methanol	Sigma, and carbide phases, dendritic structure, grain size and shape
Ta - 0.5 w/o Cb	30ml $HF$ , 15ml $HNO_3$ , 30ml $HCl$	Grain size and shape

The resulting microstructures were examined with an optical microscope and selected features of each sample were photographed at various magnifications.

Representative samples from both the ground base and Skylab experiments were examined and compared using an AMR-1000 scanning electron microscope. The microstructure of the weld metal, weld interface, and base metal heat affected zone were thoroughly examined. A chemical analysis of selected features in each sample was made with the energy dispersive x-ray analyzer. Based on these studies, an in-depth analysis of the aluminum alloy, the tantalum alloy, and on selected features of the stainless steel alloy was made using the electron probe microanalyzer.

## ANALYTICAL RESULTS AND DISCUSSION

### MACROSTRUCTURE

Initially, both visual and low magnification examinations of all samples were conducted. These studies show that the weld fusion zone in the aluminum and stainless steel alloys processed aboard Skylab are broader than comparable ground base weld sections. The weld zones in the tantalum are approximately the same size, with the ground base samples having slightly larger zones. Such differences can be attributed to variations in the power profiles and beam focus, which were not controlled during the experiments.

The appearance of the etched weld sections was different for each alloy studied. The structure of the weld and weld interface of the stainless steel samples in both the ground base and Skylab samples was clearly delineated. These regions in the aluminum alloy and tantalum are not as sharply defined. The relative sharpness of the etched weld samples can be related to the thermal conductivity of the alloys and the metallurgical processes which occur in the heat affected zone.



It was further noted that two of the Skylab aluminum alloy weld sections experienced hot tearing during solidification. This effect is common to alloy systems whose composition lies between the pure metal and the eutectic composition. These effects and others will be considered further in the following sections.

## 2219-T87 ALUMINUM ALLOY

### Microhardness

For this alloy two sets of samples, each consisting of a ground base and a Skylab weld, were tested. Microhardness data were taken on both the crown and cross section in two directions, i.e., along the weld centerline and across the width of the weld. A comparison of the results obtained along the centerline of the welds show that no significant differences exist along the length of the weld or from top to bottom. The horizontal traverses indicate that the weld metal is slightly softer than the base metal and the heat affected zone. These differences were consistent when the ground base data were compared to the Skylab sample. Furthermore, the variation between sets of samples was insignificant. The most significant hardness variation was found to correspond to the region adjacent to the hot tear in the sample SL2, Fig. 1.

### Microstructure

The samples were first etched to reveal the distribution of grain size and shape. A comparison of the ground base and Skylab samples showed several differences. The crown section of sample SL1, shown in Fig. 2(a), a partial penetration sample, showed that there are three distinct types of grain structure: a fine grain chill zone adjacent to the base metal, a columnar zone of elongated grains, and an equiaxed grain zone in the center. In contrast, Fig. 2(b), the ground base partial penetration weld, has only two zones in the crown section, a fine grain chill zone, and a columnar zone. Banding was evident in both of these sections.

The cross sectional segments of these welds also revealed a major difference; the thickness of the fine grain chill zone varied in the Skylab sample but not in the ground base sample. This is illustrated in Fig. 3. The width of the zone increased as the root of the weld was approached. In all probability, this is due either to partial melting or rapid melting and cooling in this area. Also, contributing to this condition is the high thermal conductivity of the metal and use of a defocused electron beam, thus changing the power profile.

# SKY LAB WELD SAMPLE NO. 2 HORIZONTAL

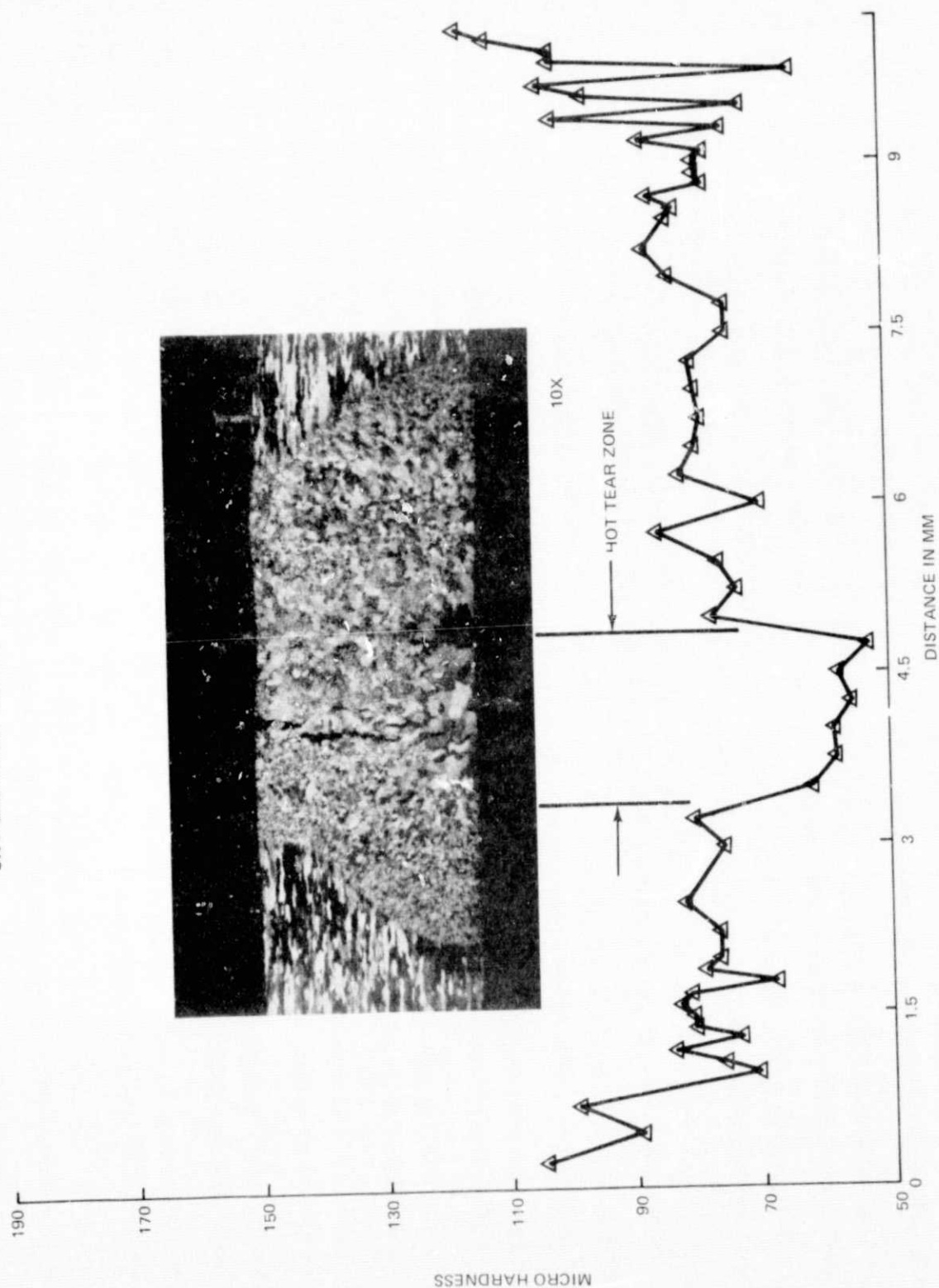
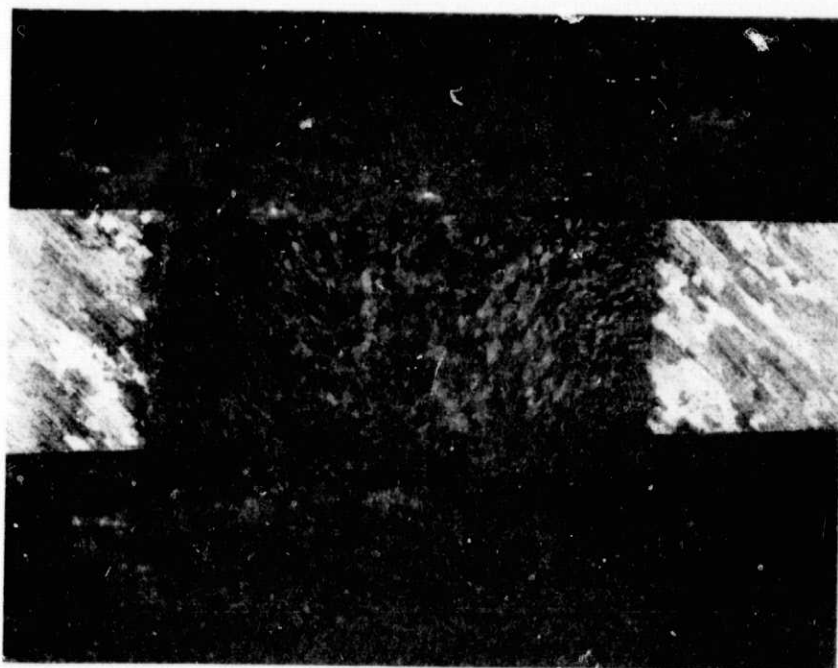
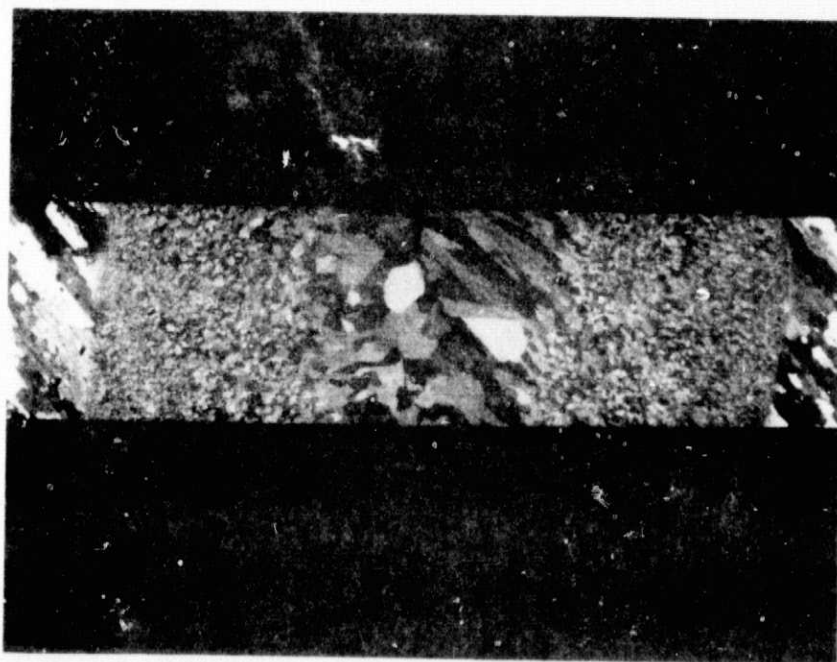


Fig. 1 Variations in Microhardness of a Weld Segment from the 2219 Aluminum Alloy Disc Processed Aboard Skylab



A. GROUND BASE

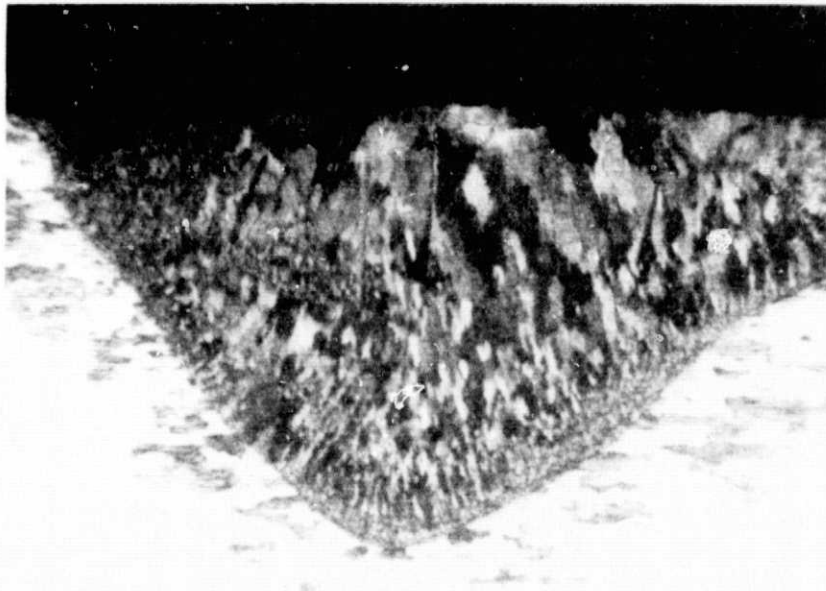
(10X)



B. SKYLAB

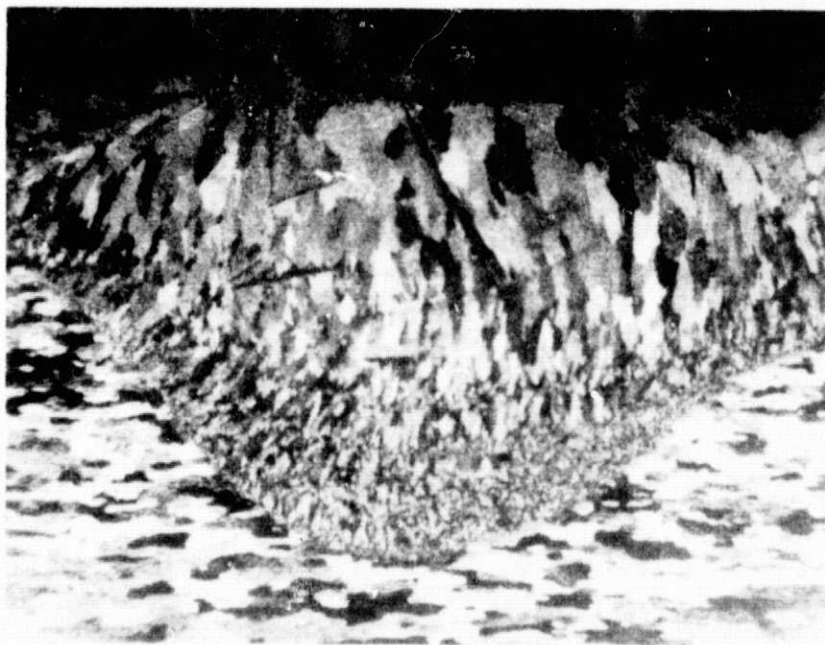
(10X)

Fig. 2 A Comparison of Growth Patterns in the Crown Sections of the Aluminum Alloy (2219) Weld



A. GROUND BASE

(100X)



B. SKYLAB

(100X)

Fig. 3 Cross Sections of the Aluminum Alloy Welds Illustrating Variation in Thickness of the Fine Grain Chill Zone

A second set of samples was also examined. In this set the ground base weld achieved almost full penetration, while the Skylab sample had full penetration and exhibited hot tears in the center of the weld. All the weld segments were found to have a uniform fine grain chill zone. The major difference found in this set of samples is the manner in which the columnar grains grow in the crown section. In the ground base sample, the growth pattern is continuously changing, i. e., it exhibits curvature as the center line is approached. The growth direction is perpendicular to the maximum temperature gradient and this condition is found when weld speeds are high. The comparable Skylab sample, on the other hand, shows little directionality in its growth and the grains are more equiaxed. In addition, there is a distinct gradient of grain size from the interface to the center line of the weld. Similarly, the dendritic patterns in the Skylab sample tend to be equiaxed and coarser than those in the ground base (Fig. 4).

When these samples were reetched to reveal the eutectic distribution and the presence of rosettes, further differences were found. The 2219 aluminum alloy is essentially an aluminum-copper binary alloy. In this system, the limit of solid solubility is in excess of 5 weight percent copper with a eutectic composition of 33 weight percent copper. When this alloy solidifies, the eutectic composition will be found in the interdendritic regions within the grains, as well as at the grain boundaries. Melting occurs in those regions where compositions at or close to the eutectic exist, when they are heated above the eutectic temperature (549° C).

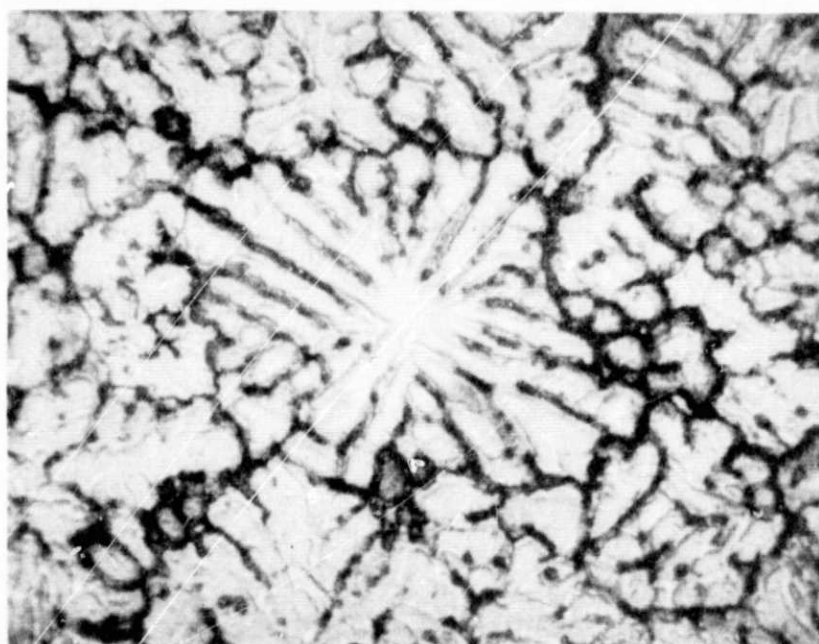
The aluminum discs used in these studies were heat treated to the T87 condition. This combination of thermal treatment and cold work should homogenize the alloy. However, an examination of all the welds shows the presence of the eutectic phase in the heat affected zone. The volume fraction of the eutectic as grain boundary melting rosettes, or distinct eutectic phase within the grains, is greater in the ground base samples than in those generated in space. Furthermore, in the ground base samples, the depth to which grain boundary melting extends is also greater. At any given distance from the weld interface, the grain boundary eutectic is thicker or coarser in these samples than for a comparable location in the space processed samples. Since the thermal conductivity of the alloy is constant in both environments, it may be concluded that the ground base welds experienced either a higher temperature or a longer time in the molten state than the Skylab welds.

Cracks or hot tears were found in both of the full penetration aluminum alloy welds which were processed in space. Comparable ground base welds did not exhibit any cracks. There are two possible explanations for these cracks or tears. Cracks in welds can be caused by thermal stresses which are generated by nonlinear temperature gradients in the



A) GROUND BASE

(600X)



B) SKYLAB

(600X)

Fig. 4 A Comparison of Dendrite Shape and Size in the Aluminum Alloy Welds

solid. The nonlinearity is due to the transient nature of the welding process. The thermal stresses generated in this manner are due in part to the alloy thermal conductivity and to the differences in contraction between the base metal and solidifying metal. The second possible reason for the cracks is hot tearing. In this case the solidification contraction is large enough to generate stresses which cause the metal to tear apart while there is still some liquid metal present. If sufficient molten metal is present, then it will flow into the hot tears and heal them. On the other hand, if the solidification process takes place very rapidly then there will be insufficient liquid to heal the tears.

### Microchemistry

Microprobe traces taken in several locations in the welds show that a high degree of solute segregation occurred during solidification. It was also observed that the degree of segregation is a function of the distance from the weld interface, i.e., it decreases with increasing distance from the interface. Furthermore, the segregation ratio is much greater in the Skylab welds than in comparable ground base samples (Figs. 5, 6).

On a microscopic scale the solute distribution, as observed in these welds, is not what would be predicted based upon the nonequilibrium equation of Scheil (Ref. 4). Macro-segregation effects must be an overriding influence which modifies the local composition and gives rise to the observed distribution.

In order to understand causes of macrosegregation, fluid flow must be considered. The effect of fluid flow on solute concentration is described by the differential equation

$$\frac{\partial g_L}{\partial C_L} = - \frac{(1-\beta)}{(1-K)} \left( \frac{1 + \vec{V} \cdot \nabla T}{\epsilon} \right) \frac{g_L}{C_L} \quad (1)$$

where  $g$  = fraction of liquid,  $C$  = solute concentration in liquid,  $\beta$  = solidification shrinkage,  $k$  = equilibrium partition ratio,  $V$  = interdendritic flow velocity,  $T$  = temperature, and  $\epsilon$  = local rate of temperature change. In Eq. (1) the term  $\frac{\vec{V} \cdot \nabla T}{\epsilon}$  is a dimensionless quantity which describes the local flow velocity perpendicular to isotherms, relative to the velocity of the isotherm movement. In general, these quantities vary with time during solidification.

When Eq. (1) is considered it can be shown that when  $-\frac{\beta}{1-\beta} = \frac{\vec{V} \cdot \nabla T}{\epsilon}$  no macro-segregation occurs. However, when the flow term in Eq. (2) increases, the solute concentration is enhanced when flow occurs from cooler to hotter regions. Even small flow velocities result in significant compositional changes. For example, during the solidification of a 4.5 w/o copper-aluminum alloy, if the rate of isotherm movement is 0.01 cm/sec and the flow velocity 0.0005 cm/sec, then the final localized concentration is changed by 20%, i.e.,

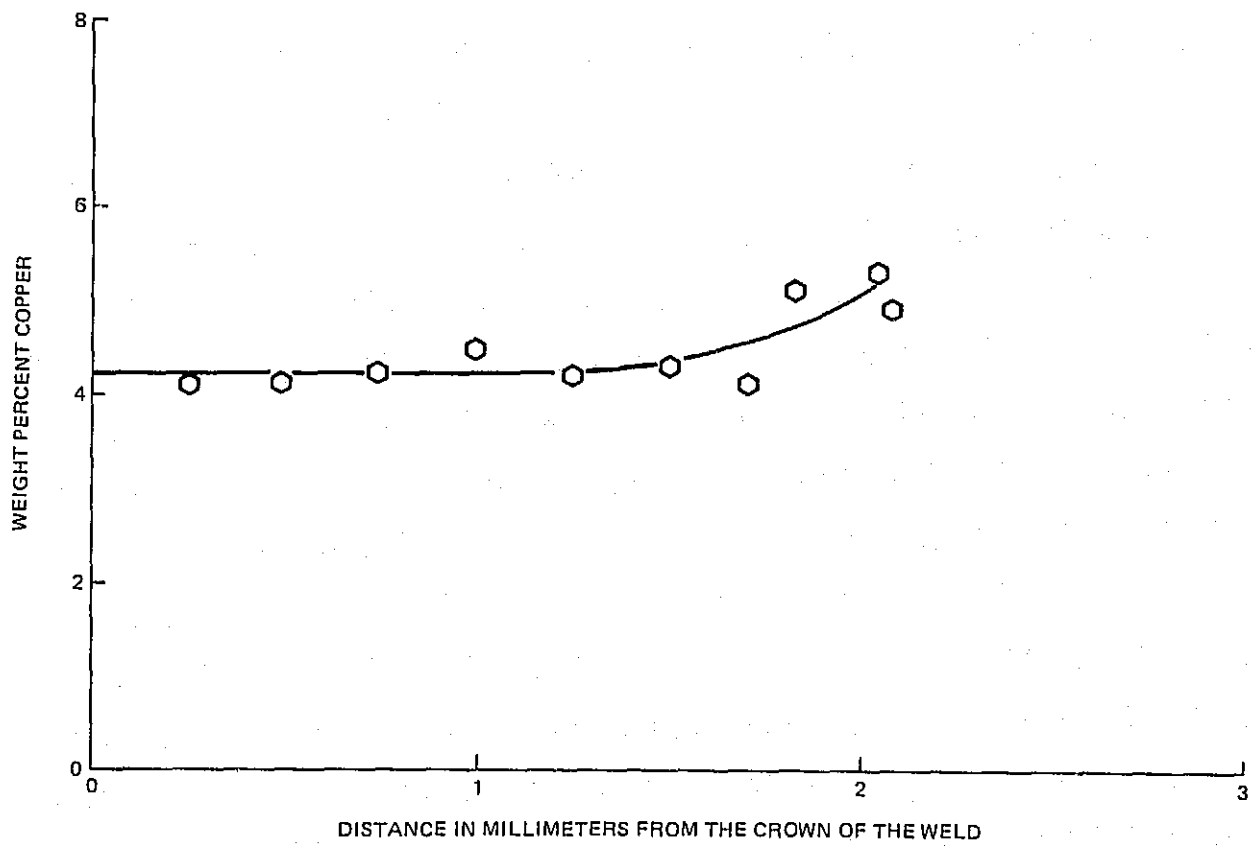


Fig. 5 Variation in the Average Copper Concentration Along the Center Line of the Ground Base Weld



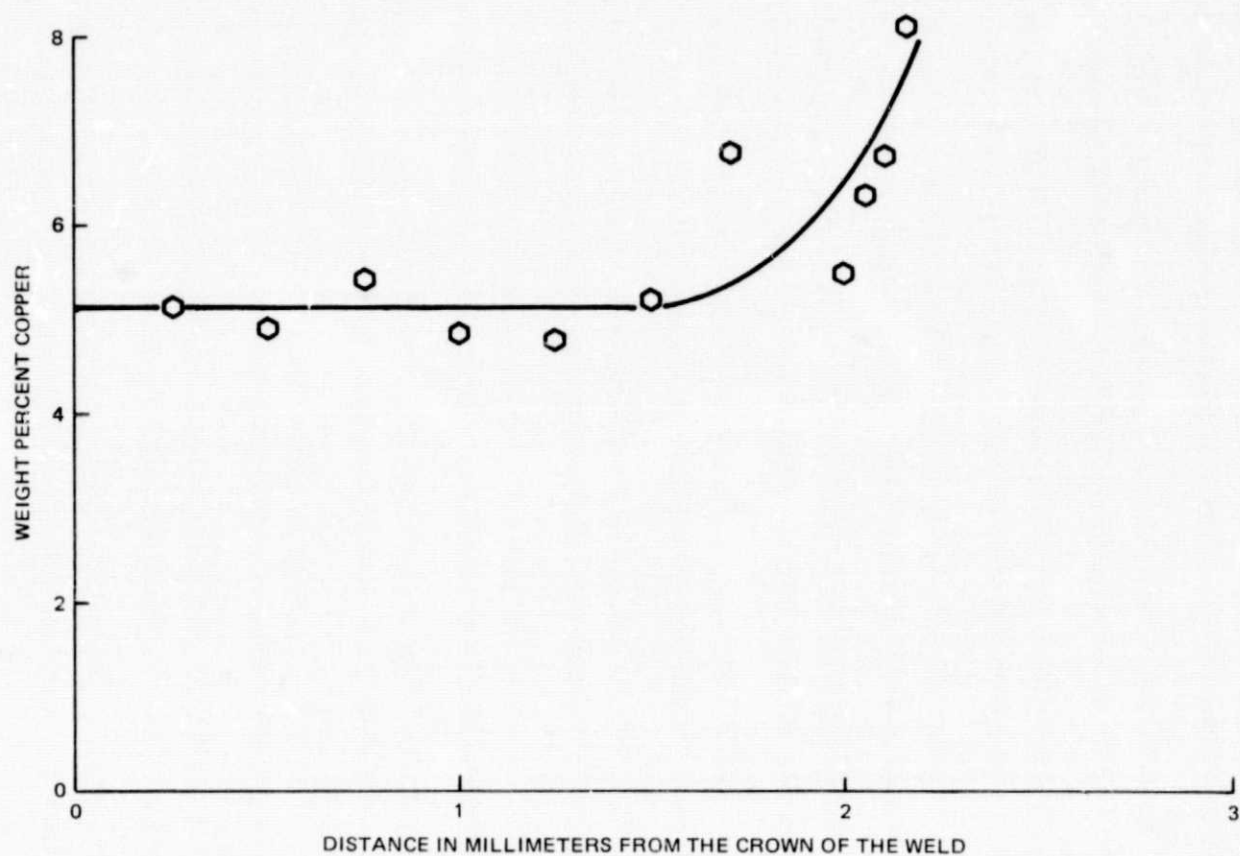


Fig. 6 Variation in the Average Copper Concentration Along the Center Line of the Skylab Weld

5.5 w/o copper. An alternate way of explaining the observed segregation pattern is to consider a change in the isotherm velocity with a constant flow velocity. Under these conditions a decreasing velocity of the isotherm will also cause an increase in the copper segregation.

The Skylab sample has been shown to have a greater degree of macrosegregation than the ground base samples. Based on the analysis above, either the flow rates must be greater or the isotherm velocity is slower. All of the commonly accepted driving forces for flow are based on either intrinsic properties of the alloy or related to gravity effects. This leaves us with second order effects, such as surface convection as the driving force, which are overshadowed in a one gravity environment.

#### TANTALUM - 0.5 W/O COLUMBIUM

##### Microhardness

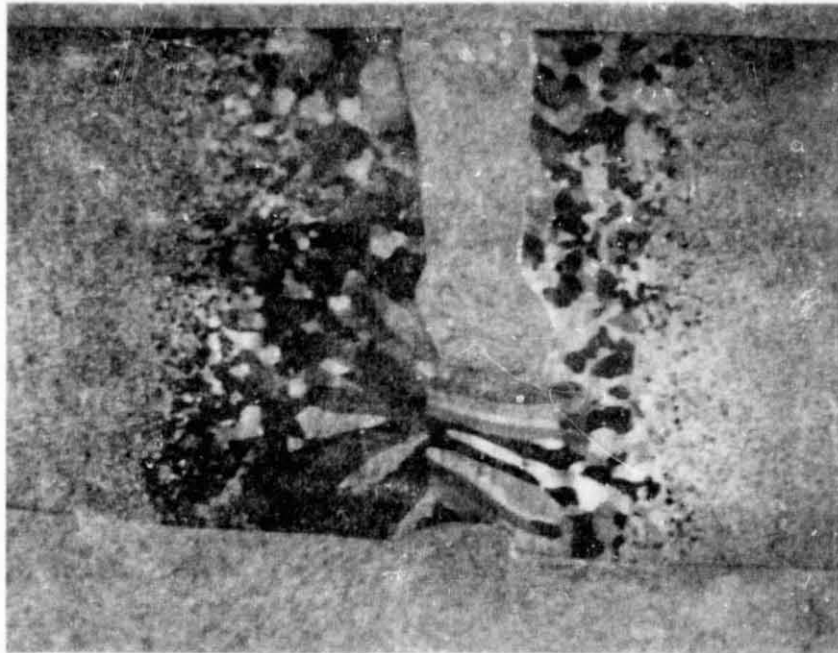
The variations in hardness across the welds has been discussed previously and will not be considered further (Ref. 5).

##### Microstructure

The crown sections of the Skylab and ground base samples exhibit two modes of grain growth. The ground base samples and the Skylab sample with the smallest cross sectional area all have columnar grains which have an epitaxial relationship with the grains at the weld interface (Fig. 7). These grains curve towards the welding direction, i.e., they grow normal to the maximum temperature gradient. This growth form is associated on earth, for a given power profile, with high welding speeds. An additional factor affecting the growth mode is the section size or the relative heat dissipating capability.

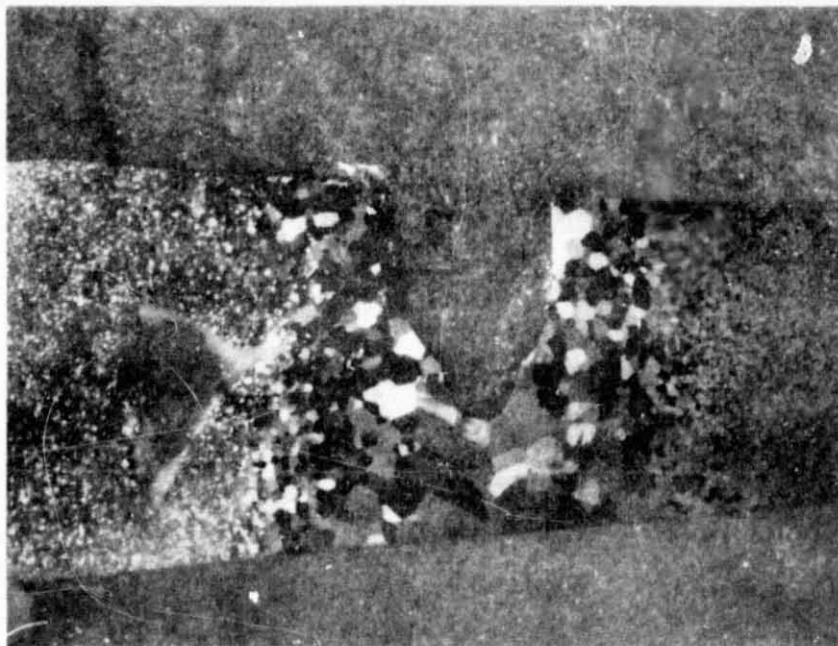
The heavier section from Skylab, however, exhibits equiaxed grains in the weld (Fig. 8). An examination of the grain structure parallel to the weld direction confirmed the equiaxed nature of the grains. Since the ground base and Skylab samples have equal cross sections, then their heat dissipating capabilities are equal. Equiaxed grains are associated with lower weld speeds or metal temperature for a given power profile. It can be concluded that either the power profile or the welding speed, or both factors, were different in the Skylab experiment than those used in the ground base experiment.

The heat affected zone in all the samples has a continuous change in grain size from the larger grains at the weld interface to the small grains in the original worked structure. This variation in grain size is due to the thermal gradient which causes recrystallization of the worked structure and subsequent grain growth. The width of this recrystallized zone is



A) GROUND BASE

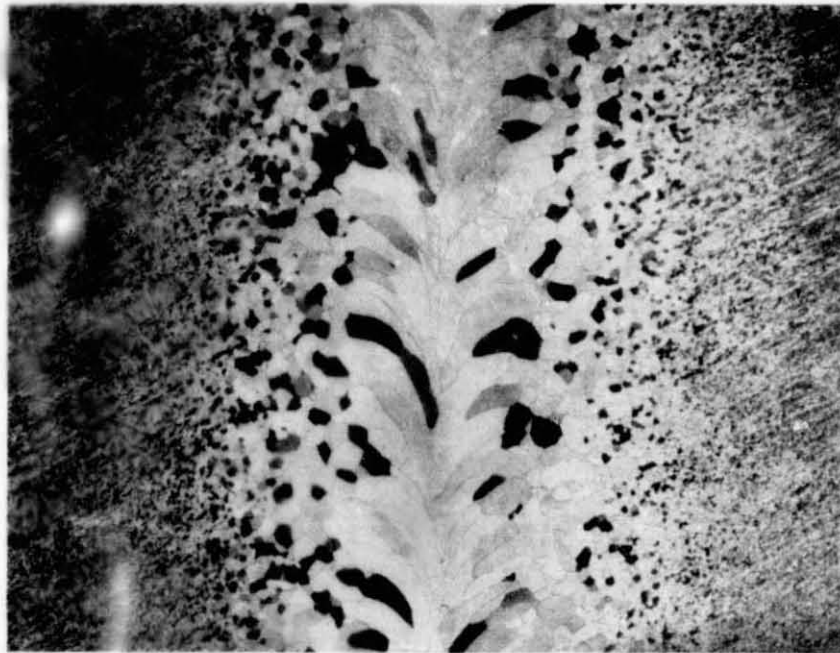
(10X)



B) SKYLAB

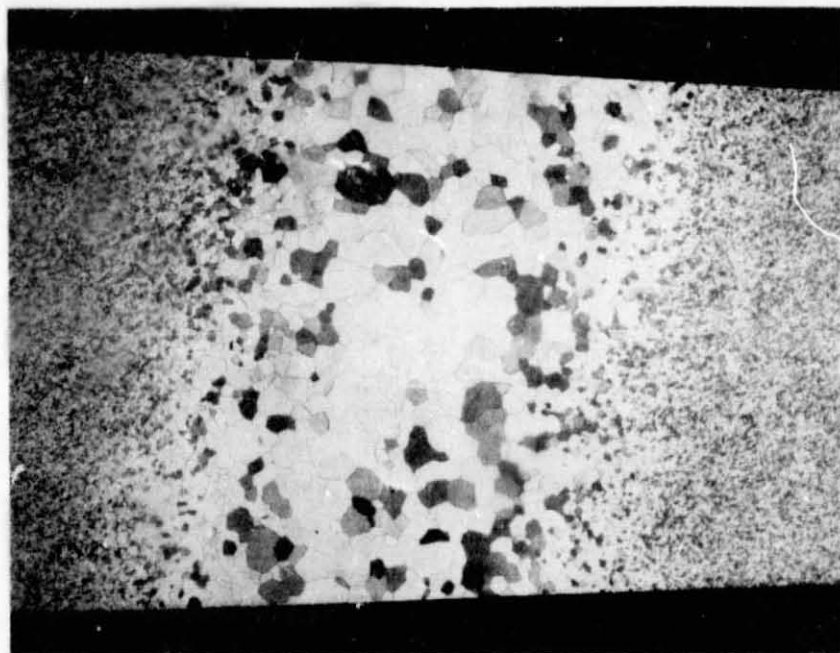
(10X)

Fig. 7 A Comparison of Solidification Patterns in the Crown Sections of Thin Cross Section Tantalum Welds



A) GROUND BASE

(10X)



B) SKYLAB

(10X)

Fig. 8 A Comparison of Solidification Patterns in the Crown Sections of Large Cross-Section Tantalum Welds

large due to the high melting point of the alloy ( $3000^{\circ}\text{C}$ ) and the relatively low recrystallization temperature ( $1350^{\circ}\text{C}$ ).

#### Microchemistry

Microprobe data taken on the ground base sample (Number 11) show that solute is rejected to the grain boundaries in the base metal, heat affected zone, and to the center line of the weld metal (Fig. 9). The comparable Skylab sample exhibited the same variations in chemistry, but only in the base metal and heat affected zone (Fig. 10). The weld metal of the flight sample shows only small variations from grain to grain. Data collected on individual grains show only small chemistry variations from edge to edge, as shown in Fig. 11. A sufficient number of counts were collected during the data generation to assure that a high degree of statistical precision was maintained. Thus, it must be concluded that the composition is relatively uniform throughout an individual grain.

#### 304L STAINLESS STEEL

#### Microhardness

Microhardness measurements on the crown section were made along the weld centerline and across the width of the weld. The data from both the ground base and Skylab samples showed no trends in either of the directions tested. Measurements were made at three different locations on the cross section segments of the welds. An examination of the data showed that no significant changes occur at the interface or at banding sites. It was concluded that the observed variations are of a statistical nature and therefore precluded any analysis.

#### Microstructure

The most striking feature of these welds is the sharply delineated weld interface. The sharpness is due to the low thermal conductivity of the alloy, as there is a sharp temperature gradient across the interface which results in a narrow heat affected zone. Due to the narrowness of the zone the surrounding microstructure in the base metal is virtually unaffected. The only observable change is the increase in the number of twins near the interface. The macrostructure of the ground base and Skylab welds reveals heavy banding and under polarized light, large columnar grains are seen.

An examination of the weld interface at high magnifications reveals that the interface is a thin ( $\sim 0.002$  mm) featureless band, whose continuity is occasionally broken by grains which grow into the melt.

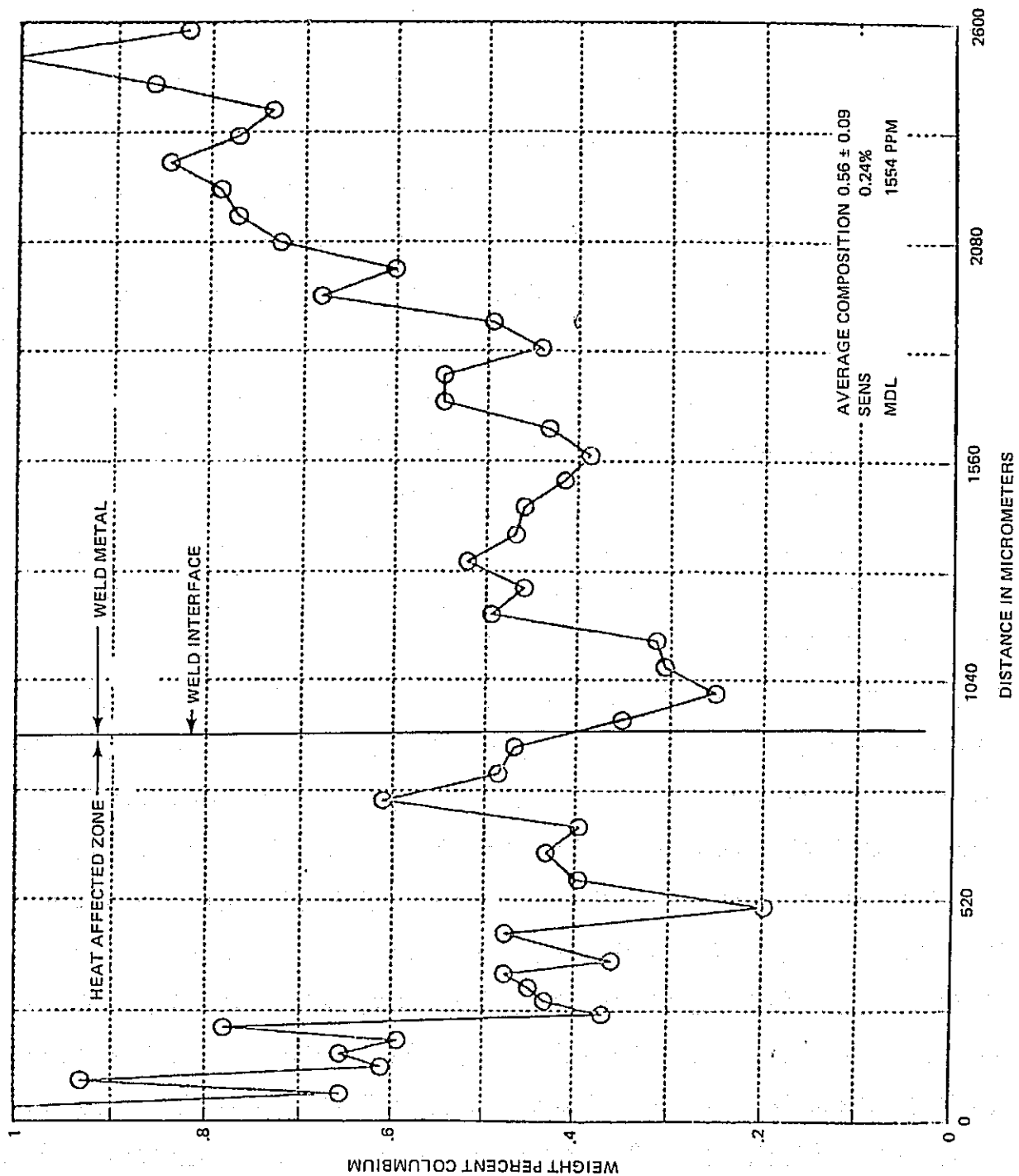


Fig. 9 Variation in Microchemistry Across the Heat Affected Zone and Weld Metal in Ground Base Sample No. 11

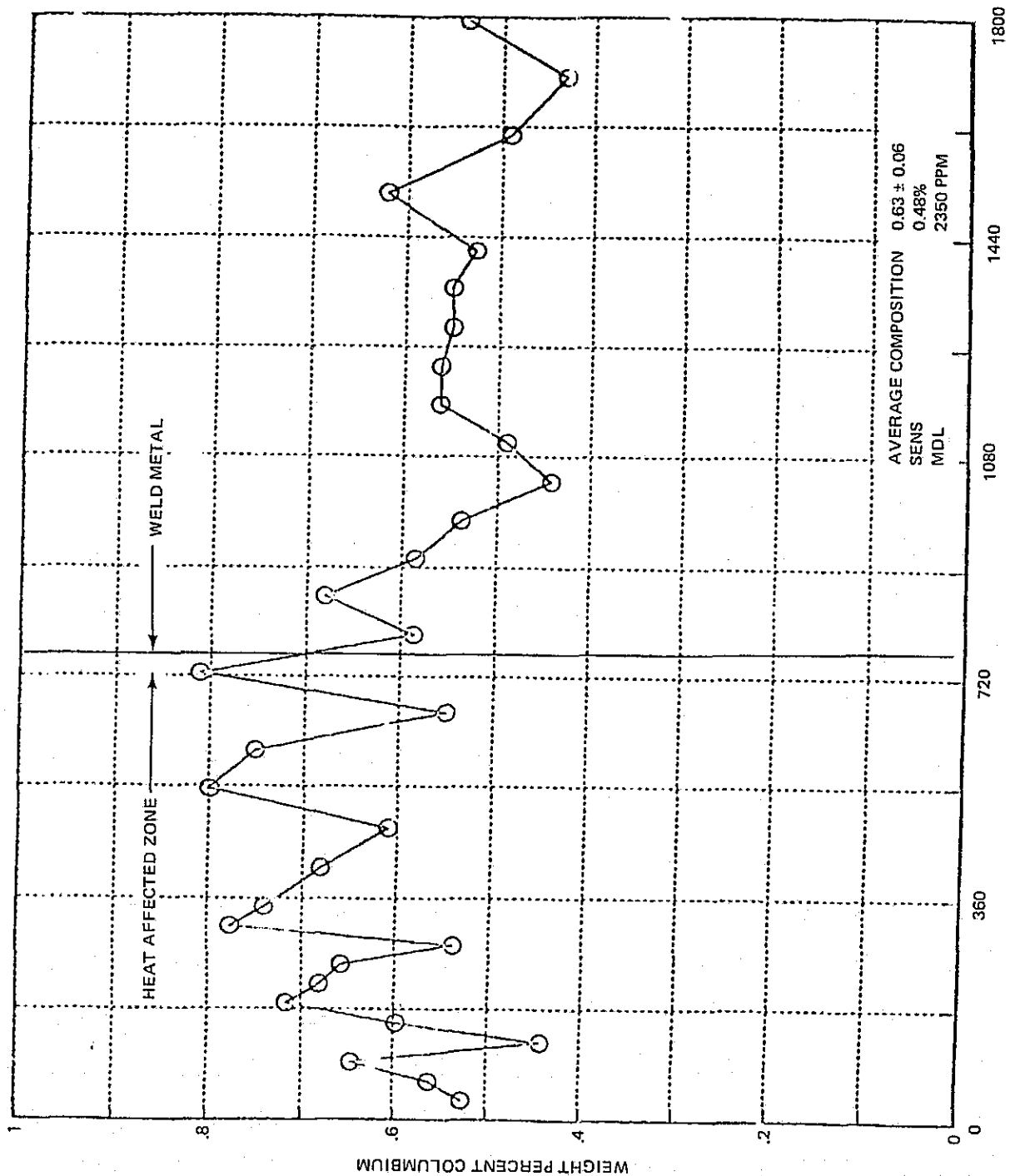


Fig. 10 Variation in Microchemistry Across the Heat Affected Zone and Weld Metal of Skylab Sample No. 11

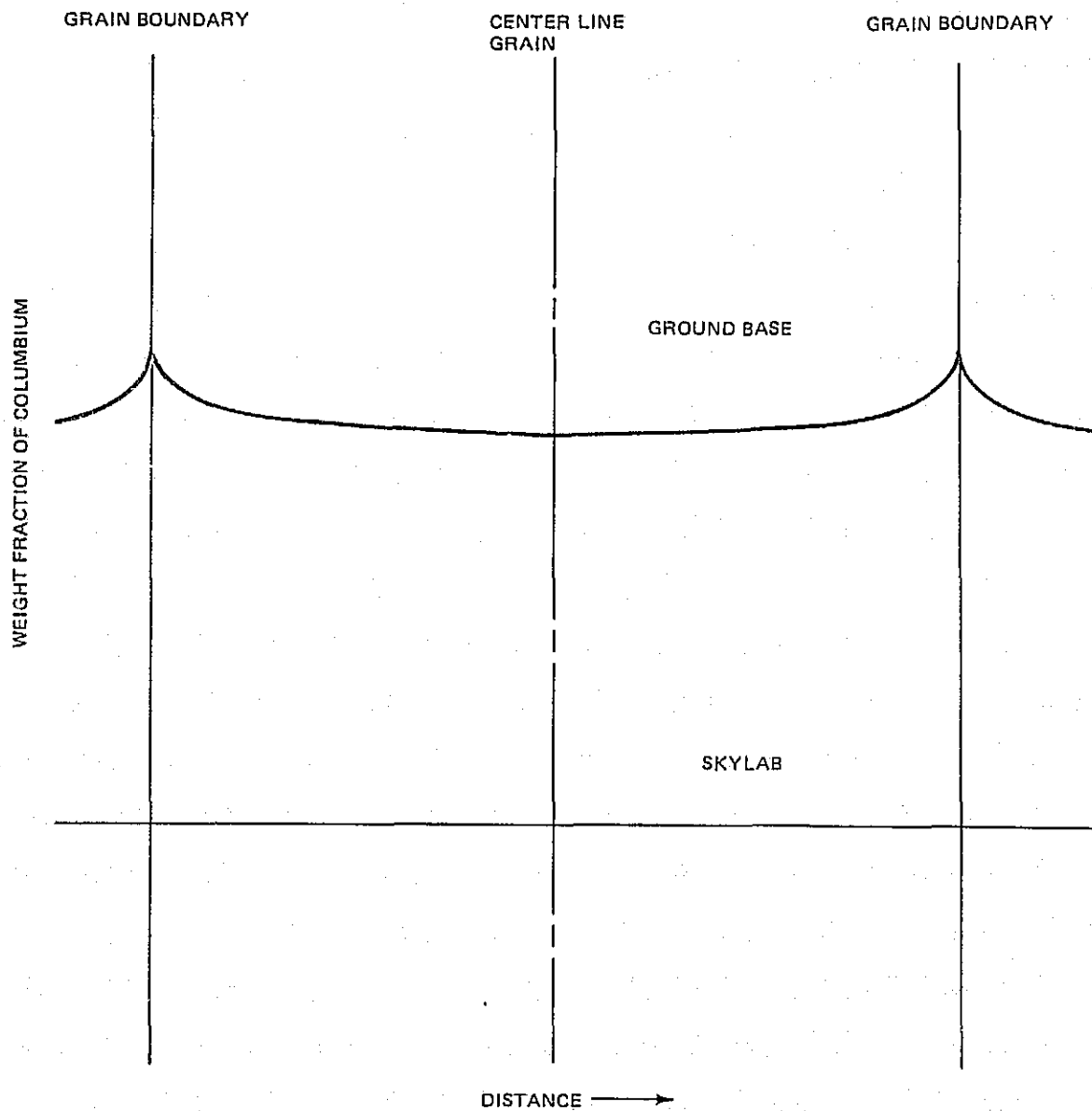


Fig. 11 Schematic of the Variations in Microchemistry of Individual Grains in the Tantalum Alloy Weld



At the termination of this initial transient the solidification mode changes to cellular growth, see Fig. 12(a). The presence of this growth form implies that constitutional supercooling of the liquid took place during solidification. During the freezing of the initial transient the conditions which are necessary to promote constitutional supercooling, such as the growth rate and temperature gradient in the liquid, are established. Once the cellular growth is initiated the intercellular regions should become enriched in solute. This growth mode is periodically interrupted by banding. These bands, which are also featureless, appear to be the result of a melt back, that changes the melting temperature and alters the conditions for cellular growth. The distribution of the elements in these two areas will be discussed in the microchemistry section. In spite of the interruption of the cellular mode by the bands, it is reinitiated and continues for some distance into the melt. Ultimately, the cellular mode becomes unstable and forms cellular dendrites. This transition is in part due to the accumulation of solute in the interdendritic regions. Once this transition occurs the cellular dendrites dominate the remainder of the solidification.

#### Microchemistry

Based on the microstructural evaluation, two areas were selected for microchemical studies. The first area encompasses the weld interface, i. e., the base metal, the initial solidification transient, and the cellular solidification zone. The second area is the region about the bands, i. e., the cellular solidification segments on either side of a band and the band itself.

An examination of Fig. 13 shows there is no change in the base metal chemistry right up to the weld interface. The chemistry of the initial transient shows a constantly increasing chromium content with a corresponding decrease in iron and nickel. The cellular structure is incubated when the values of  $G$  (temperature gradient) and  $R$  (growth rate) are established in the initial transient and when the solute is built up sufficiently in the liquid to cause constitutional supercooling. The microchemistry of the cells, as shown schematically in Fig. 13, is depleted in chromium, whereas the intercellular regions are enriched in chromium. The partitioning of one or more of the solutes in this manner would be expected when constitutional supercooling occurs.

The changes in the chemistry of the solidification process in the vicinity of the bands were examined and schematically represented in Fig. 14. As illustrated in this figure the behavior of iron and nickel is similar and opposite that of chromium. It is clear from this study that there is a zone just before the band which has an increasing chromium content in the intercellular region and a corresponding decrease in chromium within the cells. The

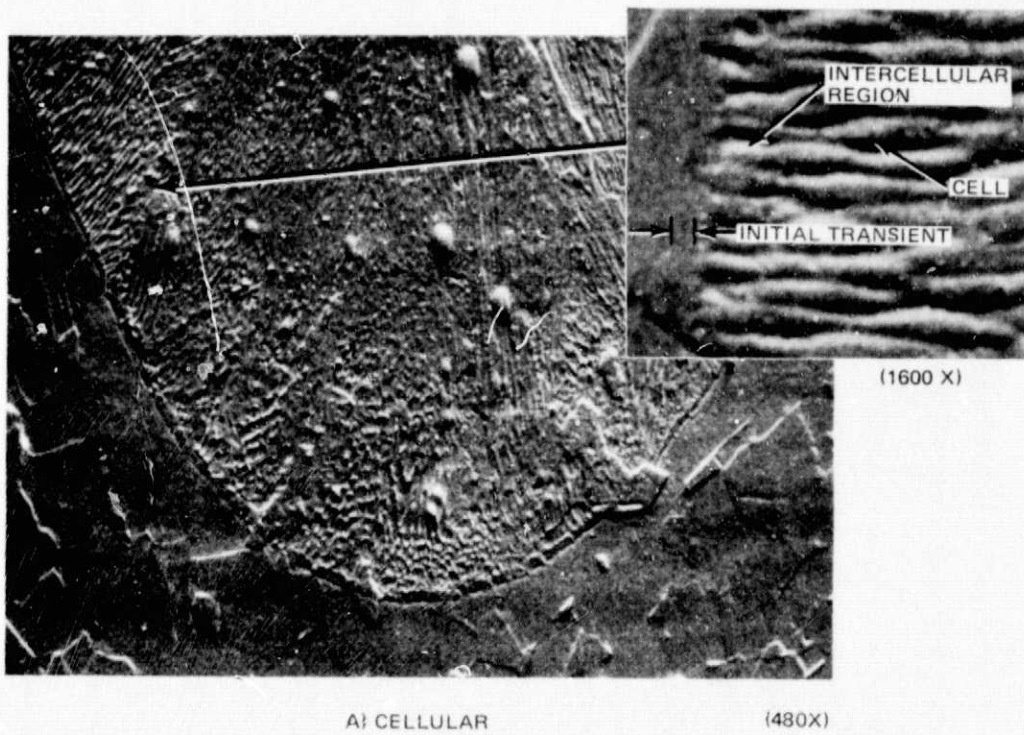


Fig. 12 Solidification Modes Found in Stainless Steel Alloy Welds A) Initial Transient and Cellular B) Cellular Dendrites

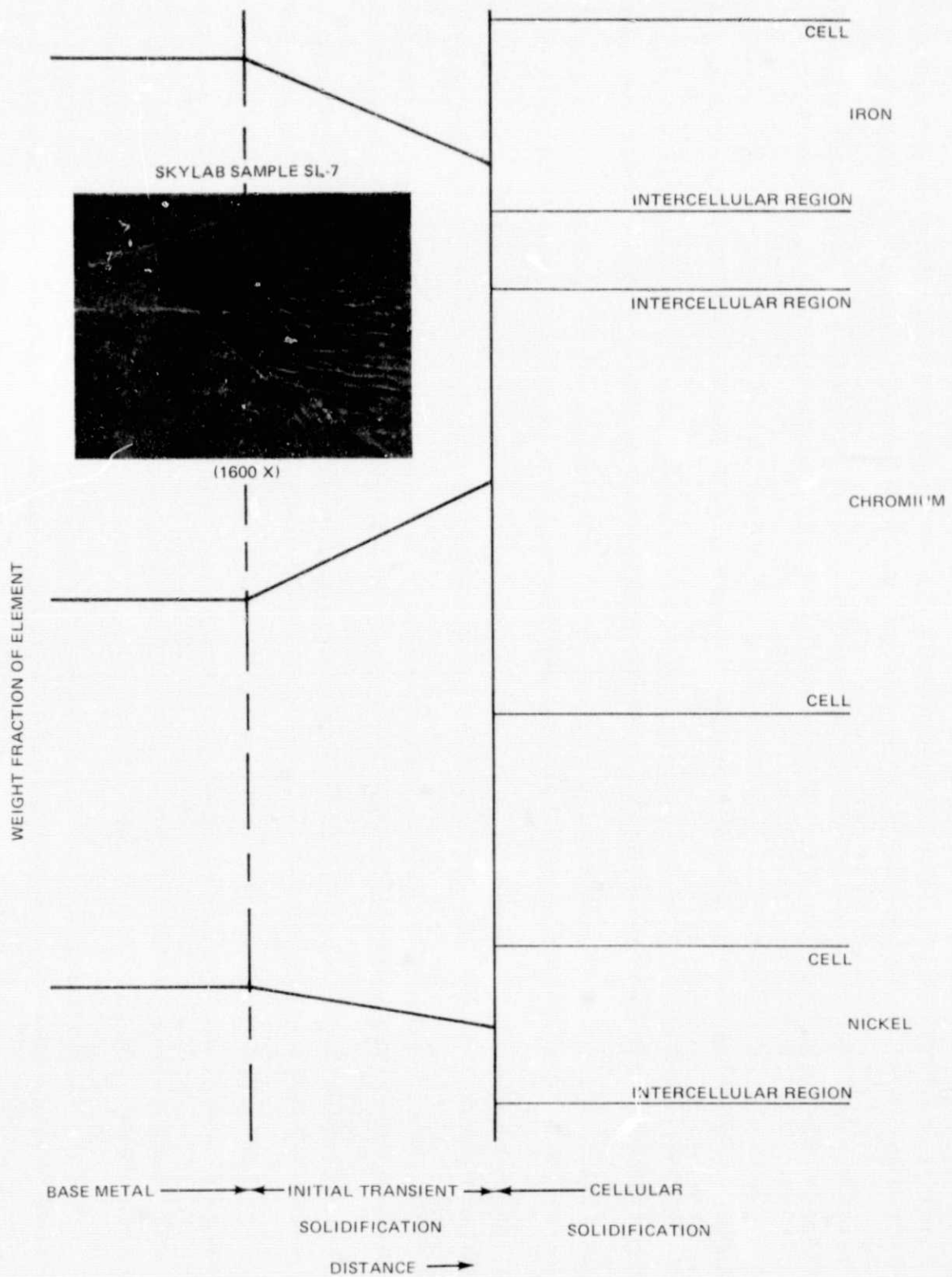


Fig. 13 Schematic of the Variations in Microchemistry at the Weld Interface in the Stainless Steel Welds

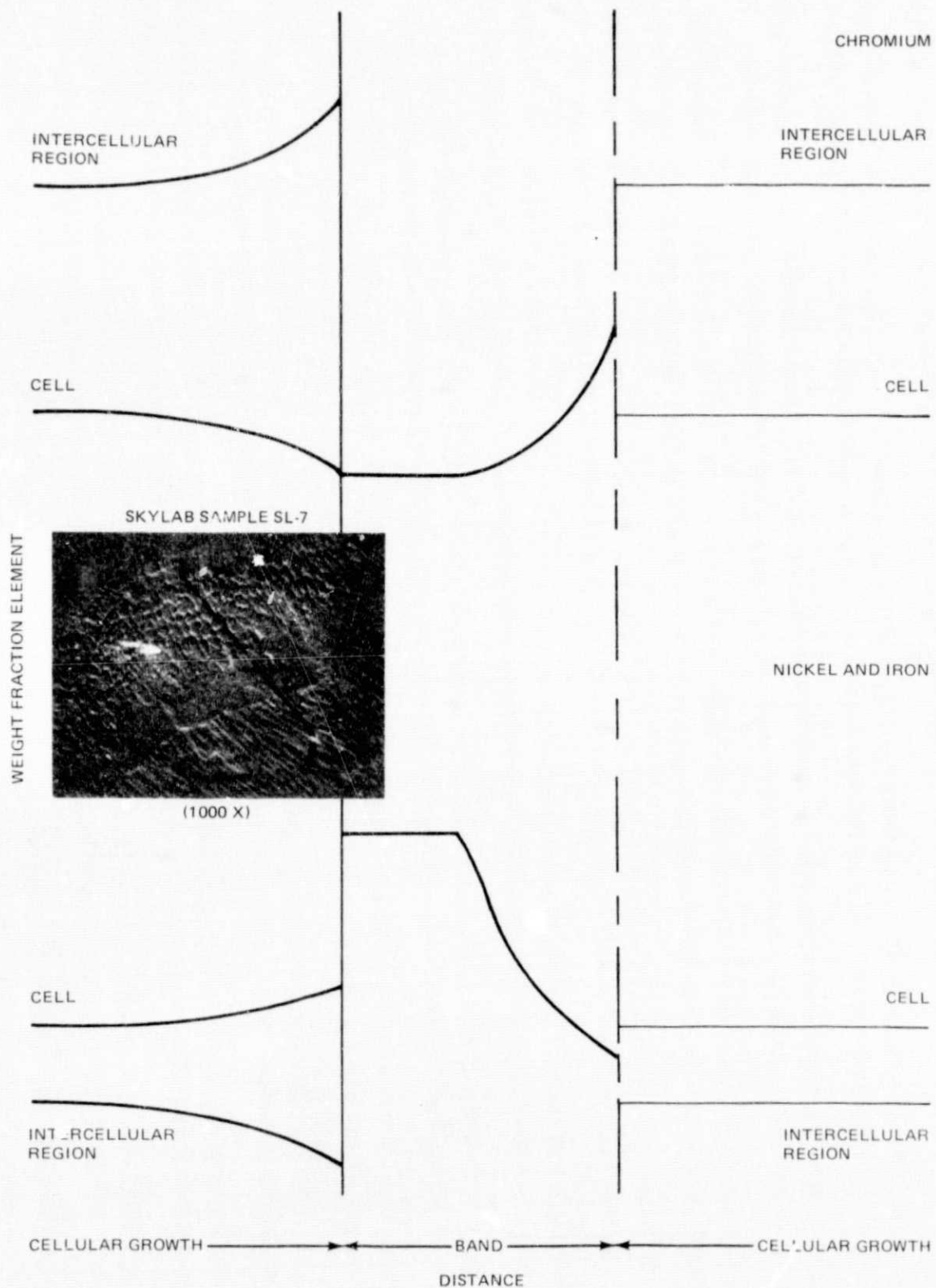


Fig. 14 Schematic of the Microchemistry Changes Across a Band in the Stainless Steel Welds

initial portion of the band is rich in iron and nickel and depleted in chromium. The latter part of the band has been found to be increasingly rich in chromium and this zone is similar to the initial transient at the weld interface. The partitioning of the solute elements in the cells and the intercellular regions is the same as found in the initial cellular solidification region. A possible explanation for this sequence is that there is an increase in the growth rate of the cells. This would result in the increased rejection of chromium and a rise in the temperature of the liquid metal due to the latent heat of fusion and the inability of the liquid to dissipate the increased heat content. The advancing cells would at some point become unstable due to their chemistry, the chemistry in the intercellular regions, the chemistry of the liquid, and the increasing temperature, thus resulting in a melt back. The liquid would now have an iron-nickel rich zone at the solid-liquid interface. When this zone resolidifies, the initial solidified material would be, as observed, iron-nickel rich. Subsequent solidification after this layer would be similar to that observed in the initial transient at the weld interface, i. e., an increase in the chromium content. The changes in microchemistry would result, in part, in reestablishing the conditions for constitutional supercooling which would eventually reinitiate cellular solidification.

#### CONCLUSIONS

This study was conducted to continue the characterization studies initiated by McKannan (Ref. 1). In these initial studies it was reported that the welds in the Skylab samples had small equiaxed grains, whereas the ground base samples contained large columnar grain.

The optical microscopy and scanning microscopy studies conducted in this study confirmed these findings and further showed that the microstructure of the heat affected zone can be correlated with the thermal conductivity of the alloy. Additional microscopy studies were conducted on the aluminum alloy fusion zones with several etchants. It was shown that differences in the size and shape of the dendrites, as well as in the volume fraction of the eutectic phase, exist between the two sets of samples and these differences could be related to the microchemistry.

Microchemical mapping of these samples revealed significant differences in the redistribution of the solute in aluminum and tantalum samples processed in space. Although not known, these studies pointed out that in order to provide a complete analysis, the thermal parameters  $G$  (thermal gradient) and  $R$  (growth rate) must be defined. Therefore, in any future experiments not only must these parameters be defined but they must also be controlled. Furthermore, these current results indicate that ordinary second order effects, such as surface convection, are the predominant driving forces in space. Any future welding

experimentation should be designed to define these forces and the conditions under which they predominate.

Finally, these results indicate that differences existed between the ground and Skylab weld parameters and that they are in part responsible for the observed differences in microstructure and microchemistry.

### FUTURE WORK

It is clear from this investigation that heat extraction and fluid flow play an important role during solidification. Most of the conventional driving forces described for flow are either intrinsic properties of the material, for example, solidification shrinkage, or gravity related, such as convection. The evidence gathered in this study indicates that flow is increased in space which results in increased segregation of the solute in the 2219 aluminum alloy. Additional experiments should be designed and conducted to determine what the driving forces are and, under what conditions they manifest themselves. Furthermore, the effect of this segregation on the mechanical properties of the materials should also be examined in order to determine what effect it will have on large structures erected in space.

### ACKNOWLEDGEMENTS

This work was partially supported by NASA Contract NAS 8-28728. We would also like to acknowledge the encouragement and support of Mr. E. C. McKannan who acted as COR for this program, Drs. D. J. Larson, C. Li, and G. Geschwind for their helpful discussions, and to Mr. C. Creter for his diligent efforts to prepare the samples.

### REFERENCES

1. McKannan, E. C., Third Space Processing Symposium, Skylab Results, NASA/MSFC M-74-5, June 1975.
2. Poorman, R. M., NASA Techn. Memo NASA TMX-64960, MSFC, Alabama, May 1975.
3. Tobin, J. M., WANL-TME-2859, Supplement to the Final Report (M551 Metals Melting) to NASA Contract NAS8-28730, June 1974.
4. Fleming, M. C., Solidification Processing, McGraw-Hill, New York 1974.
5. C.H. Li, G. Busch, and C. Creter, "M551 Metals Melting Experiment," Grumman Research Department Memorandum, RM-613, February 1976.